INFLUENCE OF IMPERFECT INTERFACE OF ANISOTROPIC THERMOMAGNETOELECTROELASTIC BIMATERIAL SOLIDS ON INTERACTION OF THIN DEFORMABLE INCLUSIONS

Heorhiy SULYM[*], Andrii VASYLYSHYN[**], Iaroslav PASTERNAK[***]

[*]Bialystok University of Technology, Wiejska Str 45C, 15-351 Bialystok, Poland
[**]Ivan Franko National University of Lviv, Universytetska Str. 1, 79000 Lviv, Ukraine
[***]Lesya Ukrainka Volyn National University, Potapova Str 9, 43025 Lutsk, Ukraine

h.sulym@pb.edu.pl, vasylyshyn.c.h@gmail.com, iaroslav.m.pasternak@gmail.com

received 12 March 2022, revised 30 May 2022, accepted 31 May 2022

Abstract: This work studies the problem of thermomagnetoelectroelastic anisotropic bimaterial with imperfect high-temperature conducting coherent interface, whose components contain thin inclusions. Using the extended Stroh formalism and complex variable calculus, the Somigliana-type integral formulae and the corresponding boundary integral equations for the anisotropic thermomagnetoelectroelastic bimaterial with high-temperature conducting coherent interface are obtained. These integral equations are introduced into the modified boundary element approach. The numerical analysis of new problems is held and results are presented for single and multiple inclusions.

Key words: anisotropic bimaterial, thermomagnetoelectroelastic, imperfect interface, high-temperature conducting, thin inclusion

1. INTRODUCTION

Pyroelectric, pyromagnetic and multifield material structures are widely used in modern engineering design, especially in the developed high-tech manufactures, devices of fine mechanics and of innovative character. These structures allow combining and redistributing the energy of four fields of different physical nature (mechanical, thermal, electrical and magnetic), and therefore have great potential for use in instrument and sensor systems, precision positioning devices, energy converters and more.

The development of such bimaterials can be provided by mechanical combination of pyroelectric (ferroelectric) and magnetostrictive (piezomagnetic) materials. As a result, a thin layer appears at the interface, which affects the temperature and stress fields in a structurally inhomogeneous solid. When modelling the effect of this layer, certain boundary conditions of imperfect thermal and magnetoelectromechanical contact of bimaterial components are used. Mainly in the scientific literature [1], [2], there are two types of imperfect thermal conditions of contact of a thin layer with the environment. These are the high- and low-temperature conducting. There are also two types of imperfect mechanical contact conditions, which are the soft and rigid interfaces. In addition, there can be present some other inhomogeneities in the structural materials (e.g. cracks, thin inclusions etc.), which can also be modelled in conditions of imperfect contact, and they should be taken into account. Thus, the development of effective methods for modelling and studying the distribution of thermal, mechanical, electric and magnetic fields in bimaterial deformable solids with an imperfect material interface and internal thin inhomogeneities is an important scientific problem with wide possibilities of practical use.

The study of bimaterial solids with defects is quite widely covered in the scientific literature. For example, in [13] the authors studied three models of interfacial cracks (electrically perfectly permeable, semi-permeable and impermeable) in piezoelectric materials using the boundary element method. The article [14] presents an analysis of problems for cracks in homogeneous piezoelectrics and at the interface of two different piezoelectric materials; the corresponding explicit analytical solutions are obtained. In [2] author uses specially designed conditions at the material boundary to model the contact surface between two anisotropic materials. Pan and Amadei in [11] developed an effective boundary-element approach to solving problems for elastic anisotropic bimaterial solids containing cracks and thin inclusions. Wang and Pan [12] constructed Green's functions for an anisotropic thermoelastic bimaterial with a Kapitza-type interface.

An effective method for solving thermomagnetoelectroelastic problems for bimaterials is an approach based on the methods of complex variable calculus and the Stroh formalism. It is widely used in the analysis of anisotropic [6], [7], piezoelectric [7], [15], [16] and magnetoelectroelastic [15] solids with through cracks and inclusions. In [3], [4], boundary integral Somilliana-type equations for the boundary-element analysis of anisotropic thermomagnetoelectroelastic bimaterial with holes, cracks and thin inclusions are obtained.

This paper expands the possibilities of the Stroh formalism-based approach for a thermomagnetoelectroelastic bimaterial solid with a high-temperature conducting interface and perfect magnetoelectromechanical contact of components that may contain thin inclusions sensitive to the influence of fields of different nature. An appropriate mathematical model has been developed. Also, there were obtained integral equations of the Somilliana-type and solved a number of problems for single and interacting inclusions.

sciendo
DOI 10.2478/ama-2022-0029

2. GOVERNING EQUATIONS OF THERMOMAGNETOELECTROELASTICITY

Consider a piecewise homogeneous anisotropic linear thermomagnetoelectroelastic medium in the reference coordinate system $Ox_1x_2x_3$. According to [6], [7] and [8], the balance equations for stress, electric displacement, magnetic induction and heat flux, as well as constitutive relations can be expressed using the complex variable calculus. The extended Stroh formalism allows to write the general solution of these equations through certain analytical functions $f(z)$ and $g(z)$ as

$$\theta = 2\mathrm{Re}\{g'(z_t)\}, \vartheta = 2k_t\mathrm{Im}\{g'(z_t)\};$$

$$\tilde{\mathbf{u}} = 2\mathrm{Re}[\mathbf{A}\mathbf{f}(z_*) + \mathbf{c}g(z_t)], \tilde{\boldsymbol{\varphi}} = 2\mathrm{Re}[\mathbf{B}\mathbf{f}(z_*) + \mathbf{d}g(z_t)];$$

$$\tilde{u}_i = u_i, \tilde{u}_4 = \phi, \tilde{u}_5 = \psi; \tilde{\sigma}_{ij} = \sigma_{ij}, \tilde{\sigma}_{4j} = D_j, \tilde{\sigma}_{5j} = B_j \ (i = 1,2,3)$$

$$\tilde{\sigma}_{i1} = -\tilde{\varphi}_{i,2}, \tilde{\sigma}_{i2} = \tilde{\varphi}_{i,1}; z_t = x_1 + p_t x_2, z_\alpha = x_1 + p_\alpha x_2; \quad (1)$$

$$h_1 = -\vartheta_{,2}, h_2 = \vartheta_{,1}; k_t = \sqrt{k_{11}k_{22} - {k_{12}}^2},$$

$$\mathbf{f}(z_*) = [F_1(z_1), F_2(z_2), F_3(z_3)]^{\mathrm{T}},$$

where σ_{ij} is a stress tensor; u_i is a displacement vector; h_i is heat flux; D_i is electric displacement; B_i is magnetic induction; q is a density of free charges; f_i is the body force; f_h is the density of distributed heat; ϕ and ψ are electric and magnetic potentials; θ is a change of temperature with respect to the reference one; k_{ij} are thermal conductivity coefficients; ϑ is heat flow function; $\mathbf{f}(z)$ is a vector of Stroh complex potentials; $g(z)$ is a temperature potential; $F_\alpha(z_\alpha)$ are certain analytical functions; and p_t is a complex constant (with a positive imaginary part), which is the root of the characteristic equation of thermal conductivity $k_{22}p_t^2 + 2k_{12}p_t + k_{11} = 0$.

Matrices $\mathbf{A} \equiv [A_{i\alpha}] = [\mathbf{a}_\alpha]$, $\mathbf{B} \equiv [b_{i\alpha}] = [\mathbf{b}_\alpha]$, constants $p_\alpha(\alpha = 1, \dots, 5)$ and vectors $\mathbf{c}$ and $\mathbf{b}$ are determined from the eigenvalue problem of the Stroh formalism [6] on the basis of elastic, piezoelectric, dielectric and piezomagnetic constants of the material.

The Stroh complex potentials, the vector-functions of displacement and stress are related by the following equations [7] :

$$\mathbf{f}(z_*) = \mathbf{B}^{\mathrm{T}}\mathbf{u} + \mathbf{A}^{\mathrm{T}}\boldsymbol{\varphi} - \mathbf{B}^{\mathrm{T}}\mathbf{u}^t - \mathbf{A}^{\mathrm{T}}\boldsymbol{\varphi}^t,$$
$$\mathbf{u}^t = 2\mathrm{Re}\{\mathbf{c}g(z_t)\}, \boldsymbol{\varphi}^t = 2\mathrm{Re}\{\mathbf{d}g(z_t)\}. \quad (2)$$

Function $g'(z_t)$, temperature and heat flux function are related as

$$g'(z_t) = \frac{1}{2}\left(\theta + i\frac{\vartheta}{k_t}\right). \quad (3)$$

3. FORMULATION OF THE PROBLEM

Consider the problem of thermal conductivity and deformation for an anisotropic thermomagnetoelectroelastic bimaterial medium with inclusions. It consists of two thermomagnetoelectroelastic anisotropic half-spaces, which are separated by a surface $x_2 = 0$ and contains cylindrical holes parallel to the x_3 axis on the surface of which arbitrary independent mechanical and thermal boundary conditions are given (Fig.1). In this case, it suffices to consider the temperature and thermomagnetoelectroelastic state in an arbitrary cross-section K which is perpendicular to x_3.

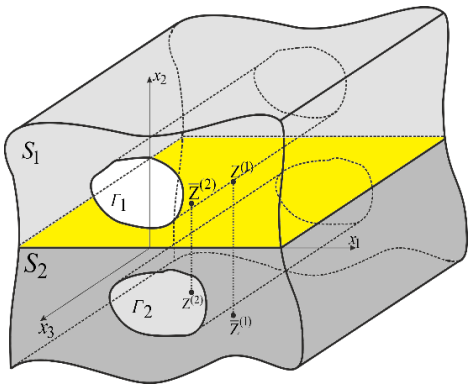

Fig. 1. Geometric scheme of a plane problem for a thermomagnetoelectroelastic anisotropic bimaterial medium

At the interface, the conditions of imperfect thermal contact in the form of a high-temperature conducting interface

$$\vartheta^{(1)}(x_1, x_2)|_{x_2=0} = \vartheta(x_1) + \mu_0\theta_{,1}(x_1), \mu_0 = 2h^{int}k_{22}^{int},$$
$$\vartheta^{(2)}(x_1, x_2)|_{x_2=0} = \vartheta(x_1), \quad (4)$$

$$\theta^{(1)}(x_1, x_2)|_{x_2=0} = \theta^{(2)}(x_1, x_2)|_{x_2=0} = \theta(x_1), \forall x_2 = 0; \quad (5)$$

and the conditions of perfect magnetoelectromechanical contact of components are given

$$\tilde{\mathbf{u}}^{(1)}(x_1, x_2)|_{x_2=0} = \tilde{\mathbf{u}}^{(2)}(x_1, x_2)|_{x_2=0} = \tilde{\mathbf{u}}(x_1), \quad (6)$$

$$\tilde{\boldsymbol{\varphi}}^{(1)}(x_1, x_2)|_{x_2=0} = \tilde{\boldsymbol{\varphi}}^{(2)}(x_1, x_2)|_{x_2=0} = \tilde{\boldsymbol{\varphi}}(x_1), \forall x_2 = 0. \quad (7)$$

Here, superscripts 1 and 2 are used to denote the values of the fields acting in half-spaces S_1 and S_2, respectively. A thin intermediate layer is removed from consideration. Each half-space contains a system of smooth closed contours $\Gamma_1 = \cup_i \Gamma_i^{(1)}$ and $\Gamma_2 = \cup_i \Gamma_i^{(2)}$. On them, it is possible to set various thermal or mechanical boundary conditions.

To derive the integral formulas for the Stroh complex potentials, we use the Cauchy integral formula [5]:

$$\frac{1}{2\pi i}\int_{\partial S}\frac{\phi(\tau)d\tau}{\tau - z} = \begin{cases}\phi(z) & \forall z \in S,\\ 0 & \forall z \notin S.\end{cases} \quad (8)$$

It outlines the relationship between the values of an arbitrary complex function (analytic in $z \in S$) at the boundary ∂S of the domain S outside and inside it. The function $\phi(z)$ is assumed to have no poles in $z \in S$. Here $\tau, z \in \mathbb{C}$ are complex variables that characterise the location of the source points and the field, respectively. Also, in Eq. (8) it is assumed that when the domain S is infinite, then the function $\phi(\tau)$ should vanish at $z \to \infty$.

4. DERIVATION OF INTEGRAL REPRESENTATIONS FOR BIMATERIAL WITH IMPERFECT THERMAL CONTACT OF COMPONENTS

4.1. Thermal conductivity

The problem of thermal conductivity is linear. Its solution can be represented as a superposition of homogeneous and perturbed solutions. Homogeneous solutions $g_{1\infty}(z_t^{(1)})$ and $g_{2\infty}(z_t^{(2)})$ satisfy Eq. (3). The perturbed solutions are caused by the presence of contours Γ_1 and Γ_2 and certain boundary conditions set on them.

Let us write the Cauchy formulas for the components of the bimaterial as follows:

$$\forall \mathrm{Im}\left(z_t^{(1)}\right) > 0,$$

$$g_1'\left(z_t^{(1)}\right) = \frac{1}{2\pi i}\int_\Gamma \frac{g_1'\left(\tau_t^{(1)}\right)d\tau_t^{(1)}}{\tau_t^{(1)} - z_t^{(1)}} + \frac{1}{2\pi i}\int_{-\infty}^{\infty} \frac{g_1'(x_1)dx_1}{x_1 - z_t^{(1)}}, \tag{9.1}$$

$$\forall \mathrm{Im}\left(z_t^{(2)}\right) < 0,$$

$$g_2'\left(z_t^{(2)}\right) = \frac{1}{2\pi i}\int_\Gamma \frac{g_2'\left(\tau_t^{(2)}\right)d\tau_t^{(2)}}{\tau_t^{(2)} - z_t^{(2)}} + \frac{1}{2\pi i}\int_{-\infty}^{\infty} \frac{g_2'(x_1)dx_1}{x_1 - z_t^{(2)}}. \tag{9.2}$$

Using the conditions of imperfect thermal contact, Eq. (3) can be written as

$$g_1'(x_1) = \frac{1}{2\pi}\left(\theta(x_1) + \frac{i}{k_t^{(1)}}\vartheta(x_1) + \frac{i\mu_0}{k_t^{(1)}}\theta_{,1}(x_1)\right); \tag{9.3}$$

$$g_2'(x_1) = \frac{1}{2\pi}\left(\theta(x_1) + \frac{i}{k_t^{(2)}}\vartheta(x_1)\right). \tag{9.4}$$

Thus, we substitute now Eqs (9.3) and (9.4) into Eqs (9.1) and (9.2), respectively

$$g_1'\left(z_t^{(1)}\right) = \frac{1}{2\pi i}\int_\Gamma \frac{g_1'\left(\tau_t^{(1)}\right)d\tau_t^{(1)}}{\tau_t^{(1)} - z_t^{(1)}} + \frac{1}{2\pi i}\left(\frac{1}{2}\int_{-\infty}^{\infty} \frac{\theta(x_1)dx_1}{x_1 - z_t^{(1)}} + \frac{i}{2k_t^{(1)}}\int_{-\infty}^{\infty} \frac{\vartheta(x_1)dx_1}{x_1 - z_t^{(1)}} + \frac{i}{2k_t^{(1)}}\int_{-\infty}^{\infty} \frac{\mu_0\theta_{,1}(x_1)dx_1}{x_1 - z_t^{(1)}}\right);$$

$$g_2'\left(z_t^{(2)}\right) = \frac{1}{2\pi i}\int_\Gamma \frac{g_2'\left(\tau_t^{(2)}\right)d\tau_t^{(2)}}{\tau_t^{(2)} - z_t^{(2)}} + \frac{1}{2\pi i}\left(\frac{1}{2}\int_{-\infty}^{\infty} \frac{\theta(x_1)dx_1}{x_1 - z_t^{(2)}} + \frac{i}{2k_t^{(2)}}\int_{-\infty}^{\infty} \frac{\vartheta(x_1)dx_1}{x_1 - z_t^{(2)}}\right).$$

Excluding integrals along the interface of half-spaces we obtain

$$g_1'\left(z_t^{(1)}\right) = \frac{1}{2\pi i}\left[q_t^{(1)}\left(z_t^{(1)}\right) + \bar{q}_t^{(1)}\left(z_t^{(1)}\right) - \frac{(1+K)}{\beta_1}\bar{e}_t^{(1)}\left(\beta_1; z_t^{(1)}\right) + \frac{(1-K)}{\beta_1}e_t^{(2)}\left(\beta_1; z_t^{(1)}\right)\right]. \tag{10}$$

$$g_2'\left(z_t^{(2)}\right) = \frac{1}{2\pi i}\left[q_t^{(2)}\left(z_t^{(2)}\right) + \bar{q}_t^{(2)}\left(z_t^{(2)}\right) + \frac{(1+K)}{\beta_2}e_t^{(1)}\left(\beta_2; z_t^{(2)}\right) - \frac{(1-K)}{\beta_1}\bar{e}_t^{(2)}\left(\beta_2; z_t^{(2)}\right)\right]. \tag{11}$$

Here

$$q_t^{(i)}\left(z_t^{(j)}\right) = \int_{\Gamma_i}\frac{g_i'\left(\tau_t^{(i)}\right)d\tau_t^{(i)}}{\tau_t^{(i)} - z_t^{(j)}},\ \bar{q}_t^{(i)}\left(z_t^{(j)}\right) = \int_{\Gamma_i}\frac{\overline{g_i'\left(\tau_t^{(i)}\right)}d\bar{\tau}_t^{(i)}}{\bar{\tau}_t^{(i)} - z_t^{(j)}}.$$

$$K = \frac{k_t^{(1)} - k_t^{(2)}}{k_t^{(1)} + k_t^{(2)}};\ \frac{1}{k_t^{(1)} + k_t^{(2)}} = \frac{1+K}{2k_t^{(1)}} = \frac{1-K}{2k_t^{(2)}};$$

$$\beta_1 = -\frac{i\mu_0(1+K)}{2k_t^{(1)}},\ \beta_2 = \frac{i\mu_0(1-K)}{2k_t^{(2)}}. \tag{12}$$

$$e_t^{(k)}\left(\alpha_i; z_t^{(j)}\right) = e^{-\frac{z_t^{(j)}}{\alpha_i}}\int e^{\frac{z_t^{(j)}}{\alpha_i}} q_t^{(k)}\left(z_t^{(j)}\right)dz_t^{(j)};$$

$$\bar{e}_t^{(k)}\left(\alpha_i; z_t^{(j)}\right) = e^{-\frac{z_t^{(j)}}{\alpha_i}}\int e^{\frac{z_t^{(j)}}{\alpha_i}} \bar{q}_t^{(k)}\left(z_t^{(j)}\right)dz_t^{(j)}.$$

Thus, there are obtained integral representation for the temperature and heat flux at any point $\boldsymbol{\xi}$ bimaterial

$$\theta(\boldsymbol{\xi}) = \begin{cases} 2\mathrm{Re}\left\{g_1'\left(Z_t^{(1)}(\boldsymbol{\xi})\right)\right\}\ (\forall \boldsymbol{\xi} \in S_1), \\ 2\mathrm{Re}\left\{g_2'\left(Z_t^{(2)}(\boldsymbol{\xi})\right)\right\}(\forall \boldsymbol{\xi} \in S_2) \end{cases} =$$

$$= \int_\Gamma\left[\Theta^{\mathrm{HCI}*}(\mathbf{x}, \boldsymbol{\xi})h_n(\mathbf{x}) - \mathrm{H}^{\mathrm{HCI}*}(\mathbf{x}, \xi)\theta(\mathbf{x})\right]ds(\mathbf{x}) + \theta^\infty(\boldsymbol{\xi}); \tag{13}$$

$$h(\boldsymbol{\xi}) = \begin{cases} 2k_t^{(1)}\mathrm{Im}\left\{\left(\delta_{2i} - \delta_{1i}p_t^{(1)}\right)g_1''\left(Z_t^{(1)}(\boldsymbol{\xi})\right)\right\}\ (\forall \boldsymbol{\xi} \in S_1), \\ 2k_t^{(2)}\mathrm{Im}\left\{\left(\delta_{2i} - \delta_{1i}p_t^{(2)}\right)g_2''\left(Z_t^{(2)}(\boldsymbol{\xi})\right)\right\}\ (\forall \boldsymbol{\xi} \in S_2) \end{cases} =$$

$$= \int_\Gamma \Theta_i^{\mathrm{HCI}**}(\mathbf{x}, \boldsymbol{\xi})h_n(\mathbf{x})d\Gamma(\mathbf{x}) - \int_\Gamma \mathrm{H}_i^{\mathrm{HCI}**}(\mathbf{x}, \boldsymbol{\xi})\theta(\mathbf{x})ds(\mathbf{x}) + h_i^\infty(\boldsymbol{\xi}). \tag{14}$$

The functions $\theta^\infty(\boldsymbol{\xi})$ and $h_i^\infty(\boldsymbol{\xi})$ are homogeneous solutions for the bimaterial

$$\theta^\infty(\boldsymbol{\xi}) = \begin{cases} 2\mathrm{Re}\left\{g_{1\infty}'\left(Z_t^{(1)}(\boldsymbol{\xi})\right)\right\}\ (\forall \boldsymbol{\xi} \in S_1), \\ 2\mathrm{Re}\left\{g_{2\infty}'\left(Z_t^{(2)}(\boldsymbol{\xi})\right)\right\}(\forall \boldsymbol{\xi} \in S_2); \end{cases}$$

$$h_i^\infty(\boldsymbol{\xi}) = \begin{cases} 2k_t^{(1)}\mathrm{Im}\left\{\left(\delta_{2i} - \delta_{1i}p_t^{(1)}\right)g_{1\infty}''\left(Z_t^{(1)}(\boldsymbol{\xi})\right)\right\}\ (\forall \boldsymbol{\xi} \in S_1), \\ 2k_t^{(2)}\mathrm{Im}\left\{\left(\delta_{2i} - \delta_{1i}p_t^{(2)}\right)g_{2\infty}''\left(Z_t^{(2)}(\boldsymbol{\xi})\right)\right\}\ (\forall \boldsymbol{\xi} \in S_2). \end{cases}$$

4.2. Thermomagnetoelectric elasticity

Using Eq. (8), we write the Cauchy integral formula for vectors $\mathbf{f}^{(1)}\left(z_*^{(1)}\right)$ and $\mathbf{f}^{(2)}\left(z_*^{(2)}\right)$ of Stroh complex potentials which are analytical functions in S_1 and S_2, respectively

$$\mathbf{f}^{(1)}\left(z_*^{(1)}\right) = \frac{1}{2\pi i}\left[\int_{\Gamma_i}\langle\frac{d\tau_*^{(1)}}{\tau_*^{(1)} - z_*^{(1)}}\rangle\,\mathbf{f}^{(1)}\left(\tau_*^{(1)}\right) + \int_{-\infty}^{\infty}\langle\frac{dx_1}{x_1 - z_*^{(1)}}\rangle\,\mathbf{f}^{(1)}(x_1)\right],$$

$$\mathbf{f}^{(2)}\left(z_*^{(2)}\right) = \frac{1}{2\pi i}\left[\int_{\Gamma_i}\langle\frac{d\tau_*^{(2)}}{\tau_*^{(2)} - z_*^{(1)}}\rangle\,\mathbf{f}^{(2)}\left(\tau_*^{(2)}\right) + \int_{-\infty}^{\infty}\langle\frac{dx_1}{x_1 - z_*^{(2)}}\rangle\,\mathbf{f}^{(2)}(x_1)\right].$$

Introducing notation

$$\mathbf{q}_j\left(z_\beta^{(i)}\right) = \int_{\Gamma_i}\langle\frac{d\tau_*^{(j)}}{\tau_*^{(j)} - z_\beta^{(i)}}\rangle\,\mathbf{f}^{(j)}\left(\tau_*^{(j)}\right),$$

$$\bar{\mathbf{q}}_j\left(z_\beta^{(i)}\right) = \int_{\Gamma_i}\langle\frac{d\bar{\tau}_*^{(j)}}{\bar{\tau}_*^{(j)} - z_\beta^{(i)}}\rangle\,\bar{\mathbf{f}}^{(j)}\left(\tau_*^{(j)}\right), \tag{15}$$

we rewrite them in the form of

$$\mathbf{f}^{(1)}\left(z_*^{(1)}\right) = \frac{1}{2\pi i}\left[\mathbf{q}_1\left(z_*^{(1)}\right) + \int_{-\infty}^{\infty}\langle\frac{dx_1}{x_1 - z_*^{(1)}}\rangle\,\mathbf{f}^{(1)}(x_1)\right],$$

$$0 = \bar{\mathbf{q}}_1\left(z_*^{(1)}\right) + \int_{-\infty}^{\infty}\langle\frac{1}{x_1 - z_*^{(1)}}\rangle\,\bar{\mathbf{f}}^{(1)}(x_1)dx_1,$$

$$0 = \mathbf{q}_1\left(z_*^{(2)}\right) + \int_{-\infty}^{\infty}\langle\frac{1}{x_1 - z_*^{(2)}}\rangle\,\mathbf{f}^{(1)}(x_1)dx_1; \tag{16}$$

$$\mathbf{f}^{(2)}\left(z_*^{(2)}\right) = \frac{1}{2\pi i}\left[\mathbf{q}_2\left(z_*^{(2)}\right) + \int_{-\infty}^{\infty}\langle\frac{1}{x_1 - z_*^{(2)}}\rangle\,\mathbf{f}^{(2)}(x_1)dx_1\right],$$

$$0 = \bar{\mathbf{q}}_2\left(z_*^{(2)}\right) - \int_{-\infty}^{\infty}\langle\frac{1}{x_1 - z_*^{(2)}}\rangle\,\bar{\mathbf{f}}^{(2)}(x_1)dx_1,$$

$$0 = \mathbf{q}_2\left(z_*^{(1)}\right) - \int_{-\infty}^{\infty}\langle\frac{1}{x_1 - z_*^{(1)}}\rangle\,\mathbf{f}^{(2)}(x_1)dx_1. \tag{17}$$

Excluding from Eqs (16) and (17) integrals along the interface of half-spaces using the Stroh orthogonality conditions we obtain

$$\mathbf{f}^{(1)}\left(z_*^{(1)}\right) = \frac{1}{2\pi i}\left[\mathbf{q}_1\left(z_*^{(1)}\right) + \sum_{\beta=1}^{5}\mathbf{I}_\beta\left(\mathbf{G}_1^{(1)}\bar{\mathbf{q}}_1\left(z_\beta^{(1)}\right) + \mathbf{G}_2^{(1)}\mathbf{q}_2\left(z_\beta^{(1)}\right)\right) + \langle\bar{Q}_t^{(1)}\left(z_t^{(1)}\right)\rangle\,\boldsymbol{\delta}_1^{(1)} + \langle Q_t^{(2)}\left(z_t^{(1)}\right)\rangle\,\boldsymbol{\delta}_2^{(1)} + \langle\bar{e}_t^{(1)}\left(\beta_1; z_t^{(1)}\right)\rangle\,\mathbf{X}_1^{(1)} + \langle e_t^{(2)}\left(\beta_1; z_t^{(1)}\right)\rangle\,\mathbf{X}_2^{(1)}\right]. \tag{18}$$

Here

$$\mathbf{X}_1^{(1)} = -\boldsymbol{\delta}_1^{(1)} - 2ik_t^{(1)}\left(\mathbf{G}_1^{(1)}\bar{\boldsymbol{\mu}}_1 - \boldsymbol{\mu}_1\right),$$

$$\mathbf{X}_2^{(1)} = -\boldsymbol{\delta}_2^{(1)} + 2ik_t^{(2)}\left(\mathbf{G}_2^{(1)}\boldsymbol{\mu}_2\right).$$

$$\boldsymbol{\delta}_1^{(1)} = -(1+K)\left(\mathbf{G}_2^{(1)}\lambda_2 - \mathbf{G}_1^{(1)}\bar{\lambda}_1 - \lambda_1\right) + ik_t^{(2)}(1+K)\left(\mathbf{G}_2^{(1)}\mu_2 - \mathbf{G}_1^{(1)}\bar{\mu}_1 - \mu_1\right),$$

$$\boldsymbol{\delta}_2^{(1)} = (1-K)\left(\mathbf{G}_2^{(1)}\lambda_2 - \mathbf{G}_1^{(1)}\bar{\lambda}_1 - \lambda_1\right) + ik_t^{(2)}(1+K)\left(\mathbf{G}_2^{(1)}\mu_2 - \mathbf{G}_1^{(1)}\bar{\mu}_1 - \mu_1\right).$$

$$\mathbf{G}_1^{(1)} = -\left[\mathbf{A}_1^{\mathrm{T}}(\bar{\mathbf{A}}_1\bar{\mathbf{B}}_1^{-1} - \mathbf{A}_2\mathbf{B}_2^{-1})^{-\mathrm{T}}\bar{\mathbf{B}}_1^{-\mathrm{T}} + \mathbf{B}_1^{\mathrm{T}}(\bar{\mathbf{B}}_1\bar{\mathbf{A}}_1^{-1} - \mathbf{B}_2\mathbf{A}_2^{-1})^{-\mathrm{T}}\bar{\mathbf{A}}_1^{-\mathrm{T}}\right],$$

$$\mathbf{G}_2^{(1)} = -\left[\mathbf{A}_1^{\mathrm{T}}(\bar{\mathbf{A}}_1\bar{\mathbf{B}}_1^{-1} - \mathbf{A}_2\mathbf{B}_2^{-1})^{-\mathrm{T}}\bar{\mathbf{B}}_2^{-\mathrm{T}} + \mathbf{B}_1^{\mathrm{T}}(\bar{\mathbf{B}}_1\bar{\mathbf{A}}_1^{-1} - \mathbf{B}_2\mathbf{A}_2^{-1})^{-\mathrm{T}}\bar{\mathbf{A}}_2^{-\mathrm{T}}\right].$$

$$\mathbf{f}^{(2)}\left(z_*^{(2)}\right) = \frac{1}{2\pi i}\Big[\mathbf{q}_2\left(z_*^{(2)}\right) + \sum_{\beta=1}^{5}\mathbf{I}_\beta\left(\mathbf{G}_1^{(2)}\mathbf{q}_1\left(z_\beta^{(2)}\right) + \mathbf{G}_2^{(2)}\bar{\mathbf{q}}_2\left(z_\beta^{(2)}\right)\right) + \langle Q_t^{(1)}\left(z_t^{(2)}\right)\rangle\,\boldsymbol{\delta}_1^{(2)} + \langle \bar{Q}_t^{(2)}\left(z_t^{(2)}\right)\rangle\,\boldsymbol{\delta}_2^{(2)} + \langle e_t^{(1)}\left(\beta_2; z_t^{(2)}\right)\rangle\,\mathbf{X}_1^{(2)} + \langle \bar{e}_t^{(2)}\left(\beta_2; z_t^{(2)}\right)\rangle\,\mathbf{X}_2^{(2)}\Big]. \quad (19)$$

and

$$\mathbf{X}_1^{(2)} = -\boldsymbol{\delta}_1^{(2)} - 2ik_t^{(1)}\mathbf{G}_2^{(2)}\boldsymbol{\mu}_1,$$

$$\mathbf{X}_2^{(2)} = -\boldsymbol{\delta}_1^{(1)} + 2ik_t^{(2)}\left(\mathbf{G}_2^{(2)}\bar{\boldsymbol{\mu}}_2 - \boldsymbol{\mu}_2\right).$$

$$\boldsymbol{\delta}_1^{(2)} = -(1+K)\left(\mathbf{G}_1^{(2)}\lambda_1 - \mathbf{G}_2^{(2)}\bar{\lambda}_2 + \lambda_2\right) - ik_t^{(2)}(1+K)\left(\mathbf{G}_1^{(2)}\mu_1 - \mathbf{G}_2^{(2)}\bar{\mu}_2 + \mu_2\right),$$

$$\boldsymbol{\delta}_2^{(2)} = (1-K)\left(\mathbf{G}_1^{(2)}\lambda_1 - \mathbf{G}_2^{(2)}\bar{\lambda}_2 + \lambda_2\right) - ik_t^{(2)}(1+K)\left(\mathbf{G}_1^{(2)}\mu_1 - \mathbf{G}_2^{(2)}\bar{\mu}_2 + \mu_2\right).$$

$$\mathbf{G}_1^{(2)} = -\left[\mathbf{A}_2^{\mathrm{T}}(\mathbf{A}_1\mathbf{B}_1^{-1} - \bar{\mathbf{A}}_2\bar{\mathbf{B}}_2^{-1})^{-\mathrm{T}}\mathbf{B}_1^{-\mathrm{T}} + \mathbf{B}_2^{\mathrm{T}}(\mathbf{B}_1\mathbf{A}_1^{-1} - \bar{\mathbf{B}}_2\bar{\mathbf{A}}_2^{-1})^{-\mathrm{T}}\mathbf{A}_1^{-\mathrm{T}}\right],$$

$$\mathbf{G}_2^{(2)} = -\left[\mathbf{A}_2^{\mathrm{T}}(\mathbf{A}_1\mathbf{B}_1^{-1} - \bar{\mathbf{A}}_2\bar{\mathbf{B}}_2^{-1})^{-\mathrm{T}}\bar{\mathbf{B}}_2^{-\mathrm{T}} + \mathbf{B}_2^{\mathrm{T}}(\mathbf{B}_1\mathbf{A}_1^{-1} - \bar{\mathbf{B}}_2\bar{\mathbf{A}}_2^{-1})^{-\mathrm{T}}\bar{\mathbf{A}}_2^{-\mathrm{T}}\right].$$

The obtained (18) and (19) allow to write integral relations that relate the displacements at an arbitrary point of the thermomagnetoelectroelastic bimaterial with temperature, heat flux and displacement and traction on the contours Γ_i:

$$\mathbf{u}(\boldsymbol{\xi}) = \begin{cases} 2\mathrm{Re}\left\{\mathbf{A}_1\mathbf{f}^{(1)}\left(Z_*^{(1)}(\boldsymbol{\xi})\right) + \mathbf{c}_1 g_1\left(Z_t^{(1)}(\boldsymbol{\xi})\right)\right\} & (\forall \boldsymbol{\xi} \in S_1), \\ 2\mathrm{Re}\left\{\mathbf{A}_2\mathbf{f}^{(2)}\left(Z_*^{(2)}(\boldsymbol{\xi})\right) + \mathbf{c}_2 g_2\left(Z_t^{(2)}(\boldsymbol{\xi})\right)\right\} & (\forall \boldsymbol{\xi} \in S_2) \end{cases} =$$

$$= \mathbf{u}^{\infty}(\boldsymbol{\xi}) + \int_\Gamma [\,\mathbf{U}^{\mathrm{bm}}(\mathbf{x},\boldsymbol{\xi})\mathbf{t}(\mathbf{x}) - \mathbf{T}^{\mathrm{bm}}(\mathbf{x},\boldsymbol{\xi})\mathbf{u}(\mathbf{x}) + \mathbf{r}^{\mathrm{HCI}}(\mathbf{x},\boldsymbol{\xi})\theta(\mathbf{x}) + \mathbf{v}^{\mathrm{HCI}}(\mathbf{x},\boldsymbol{\xi})h_n(\mathbf{x})]ds(\mathbf{x}), \quad (20)$$

Also, using Eqs (18) and (19) it is possible to write similar expressions to determine the stress in an arbitrary point of thermomagnetoelectroelastic bimaterial

$$\boldsymbol{\sigma}_j(\boldsymbol{\xi}) = \begin{cases} 2\mathrm{Re}\{\mathbf{B}_1(\delta_{2j} - \delta_{1j}p_*^{(1)})\mathbf{f}'(Z_*^{(1)}(\boldsymbol{\xi})) + \\ 2\mathrm{Re}\{\mathbf{B}_2(\delta_{2j} - \delta_{1j}p_*^{(2)})\mathbf{f}'(Z_*^{(2)}(\boldsymbol{\xi})) + \\ \quad + \mathbf{d}_1(\delta_{2j} - \delta_{1j}p_t^{(1)})g_1'(Z_t^{(1)}(\boldsymbol{\xi}))\}, (\forall \boldsymbol{\xi} \in S_1) \\ \quad + \mathbf{d}_2(\delta_{2j} - \delta_{1j}p_t^{(2)})g_2'(Z_t^{(2)}(\boldsymbol{\xi}))\}, (\forall \boldsymbol{\xi} \in S_2) \end{cases} = \quad (21)$$

$$= \boldsymbol{\sigma}_j^{\infty}(\boldsymbol{\xi}) + \int_\Gamma [\,\mathbf{D}_j^{\mathrm{bm}}(\mathbf{x},\boldsymbol{\xi})\mathbf{t}(\mathbf{x})ds(\mathbf{x}) - \mathbf{S}_j^{\mathrm{bm}}(\mathbf{x},\boldsymbol{\xi})\mathbf{u}(\mathbf{x}) + \mathbf{q}_j^{\mathrm{HCI}}(\mathbf{x},\boldsymbol{\xi})\theta(\mathbf{x})ds(\mathbf{x}) + \mathbf{w}_j^{\mathrm{HCI}}(\mathbf{x},\boldsymbol{\xi})h_n(\mathbf{x})ds(\mathbf{x})]ds(\mathbf{x}).$$

According to [10], stress and displacement discontinuities in the vicinity of tips of thin inhomogeneities are characterised by generalised stress, electric displacements and magnetic induction intensity factors. They are determined by the discontinuity functions at the tip of inhomogeneity by formulas

$$\tilde{\mathbf{k}}^{(1)} = \lim_{s\to 0}\sqrt{\frac{\pi}{8s}}\mathbf{L}\cdot\Delta\tilde{\mathbf{u}}(s);\ \tilde{\mathbf{k}}^{(2)} = -\lim_{s\to 0}\sqrt{\frac{\pi s}{2}}\Sigma\tilde{\mathbf{t}}(s),$$

where $\tilde{\mathbf{k}}^{(1)} = [K_{21}, K_{11}, K_{31}, K_{41}, K_{51}]$, $\tilde{\mathbf{k}}^{(2)} = \left[K_{12}^{(2)}, K_{22}^{(2)}, K_{32}, K_{42}, K_{52}\right]$ – are the vectors of generalised stress and electric displacement intensity factors; $\mathbf{L} = -2\sqrt{-1}\mathbf{B}\mathbf{B}^{\mathrm{T}}$– the real tensor Burnett–Lotte [9]. The first two components $K_{12}^{(2)}, K_{22}^{(2)}$ of the vector $\tilde{\mathbf{k}}^{(2)}$ differ from generalised SIFs K_{12}, K_{22}, which are introduced for purely elastic problems. To find K_{12}, K_{22}, through $\tilde{\mathbf{k}}^{(2)}$ we need to use the formula $k_i^{(2)} = S_{ji}\tilde{k}_j^{(2)}$ $(i = 1,2; j = 1,\ldots,5)$.

Here $\mathbf{k}^{(2)} = [K_{22}, K_{12}]^{\mathrm{T}}$ – the vector of generalised SIF; $\mathbf{S} = \sqrt{-1}(2\mathbf{A}\mathbf{B}^{\mathrm{T}} - \mathbf{I})$ – the second real Burnett–Lotte tensor [9].

Generalised heat flux intensity factors are defined as

$$K_{h1} = -\lim_{s\to 0}\sqrt{\frac{\pi}{8s}}k_t\cdot\Delta\theta(s);\ K_{h2} = -\lim_{s\to 0}\sqrt{\frac{\pi s}{2}}\Sigma h_n(s).$$

Fields of displacements, stresses, temperatures and heat flux in the vicinity of the inclusion tip are fully characterised by generalised stress and electric displacement intensity factors and are defined by the following relationships:

$$\tilde{\mathbf{u}}(\boldsymbol{\xi}) = \sqrt{\frac{2}{\pi}}\mathrm{Im}\{\mathbf{A}\langle\sqrt{Z_*}\rangle(\sqrt{-1}\mathbf{B}^{-1}\tilde{\mathbf{k}}^{(1)} - 2\mathbf{A}^{\mathrm{T}}\tilde{\mathbf{k}}^{(2)})\},$$

$$\tilde{\boldsymbol{\varphi}}(\boldsymbol{\xi}) = \sqrt{\frac{2}{\pi}}\mathrm{Im}\{\mathbf{B}\langle\sqrt{Z_*}\rangle(\sqrt{-1}\mathbf{B}^{-1}\tilde{\mathbf{k}}^{(1)} - 2\mathbf{A}^{\mathrm{T}}\tilde{\mathbf{k}}^{(2)})\};$$

$$\theta = \frac{1}{k_t}\sqrt{\frac{2}{\pi}}\mathrm{Im}\{(K_{h1} + \sqrt{-1}K_{h2})\sqrt{Z_t}\},$$

$$\vartheta = \sqrt{\frac{2}{\pi}}\mathrm{Im}\{(\sqrt{-1}K_{h1} - K_{h2})\sqrt{Z_t}\}.$$

5. NUMERICAL EXAMPLES

The obtained integral equations are introduced into the scheme of the modified boundary elements method [17]. To solve them, the curves $\Gamma = \bigcup_j \Gamma_j$ are approximated using n rectilinear segments (boundary elements) Γ_q. At each element, three nodal points are set: one at the centre, and two others at the distance of $\frac{1}{3}$ of element length at both sides of a central node (discontinuous three-node boundary element; if the polynomial shape functions are used it is called the discontinuous quadratic boundary element [7]). The boundary functions of temperature, heat flux, displacement and stress are approximated at the element using their nodal values. This allows solving specific two-dimensional problems of thermomagnetoelectroelasticity for bimaterial solids with imperfect thermal contact of its components in the presence of inhomogeneities inside them.

Example 1. To verify the proposed numerical method, consider a test problem for finite square solid with elementary load given on its faces, which has analytic solution. To proceed with this, let us cut out a square from the upper half-space of a bimaterial solid with high-temperature conducting interface, and consider

the prismatic body of a square cross section. To model the latter, we used only 40 boundary elements. The lower boundary of the body is at a distance *r* to the interface (Fig. 2). On the upper boundary of the body it is given a temperature θ^0.

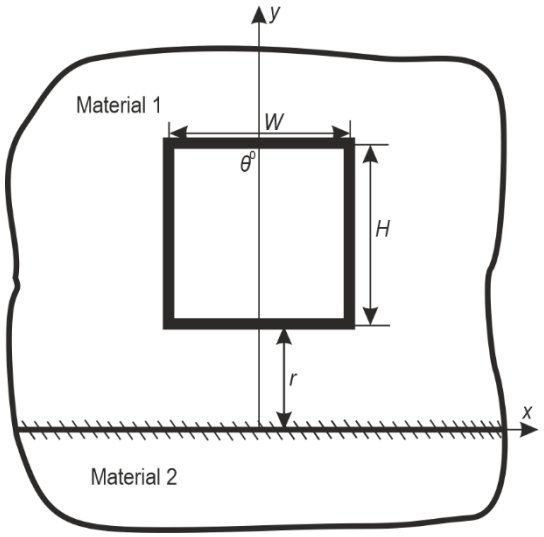

Fig. 2. Cross-sectional scheme of a thermoelastic anisotropic square body

Let us check the influence of the high-temperature conducting interface on the temperature distribution in a given finite solid. To do this, let us fix the coordinate $x = x_0 \left(x_0 \in \left[-\frac{W}{2}; \frac{W}{2}\right]\right)$ and find the temperature value at the points $y = y_0 + r(y_0 \in [0; H])$. The obtained plot shows that the temperature change is a linear function of coordinate, which is the exact analytic solution of the problem. Moreover, if one changes x_0 the resulting plot does not change, which also verifies the developed boundary element approach.

Now let us cut out the same prismatic body, with the same conditions, from the lower half-space. As in the previous case, we fix coordinate $x = x_0 \left(x_0 \in \left[-\frac{W}{2}; \frac{W}{2}\right]\right)$ and calculate the temperature value at points $y = y_0 - r(y_0 \in [-H; 0])$. The obtained schedule of temperature change is identical to the previous one, which also verifies the obtained kernels of boundary integral equations.

It should also be noted that the change in thermal conductivity of the interface does not change the temperature in these bodies. It is obvious in this case (homogeneous material) that the high thermal conductivity interface does not affect the temperature distribution in the considered finite prismatic bodies, which further verifies the obtained integral formulas and developed computational programs.

Example 2 Finally, consider the problem where the interface crosses the square solid ($W = H$), as shown in Fig. 3. The properties of the materials are the same as in the previous example. On the upper boundary of the solid, for $y = \frac{H}{2}$ the temperature is set as follows: $\theta = 4x^2/W^2$, $x \in \left[-\frac{W}{2}; \frac{W}{2}\right]$.On the bottom boundary of the cut out square a temperature $\theta^0 = 0$ is given. At the interface, the conditions of imperfect thermal contact in the form of a high-temperature conducting interface, Eqs (4) and (5), are satisfied.

In addition to the boundary elements method, another approach was used to solve the problem for their mutual verification.

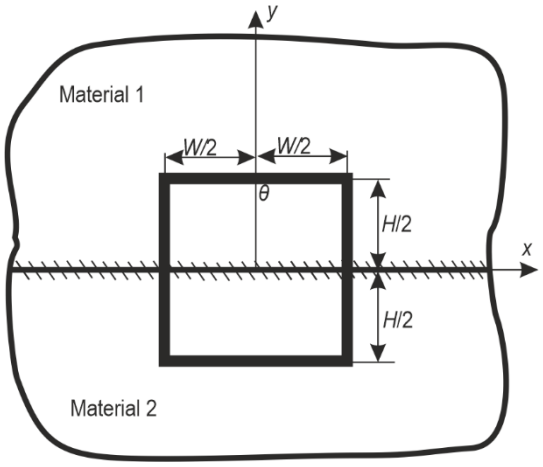

Fig. 3. Sketch of a thermoelastic anisotropic square solid with HCI

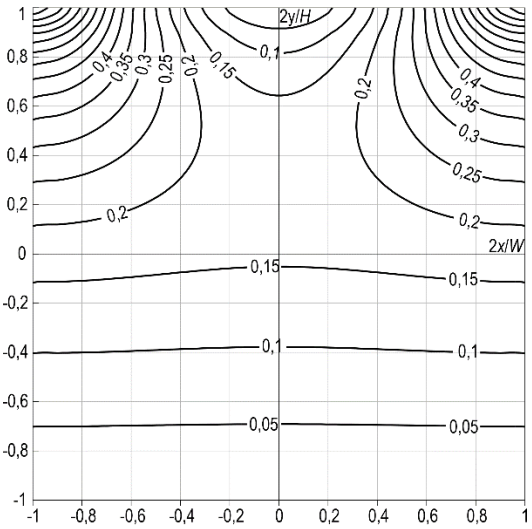

Fig. 4. Temperature change in the cross section of a square body with HCI

This approach is based on the Stroh formalism. The complex potentials (3) for a square solid with high-temperature conducting interface can be taken as the following finite sums of Laurent series, which are analytic in the selected domain

$$g_1'(z_t) = \sum_{k=0}^{N} C_k^{(1)} z_t^k, y > 0;$$
$$g_2'(z_t) = \sum_{k=0}^{N} C_k^{(2)} z_t^k, y < 0. \quad (22)$$

Here N is the number of terms. Utilising interface conditions (4) and (5) one can easily find the dependence between $C_k^{(1)}$ and $C_k^{(2)}$. After this these coefficients are determined in the following way. First, one computes the sum of squares of difference between given boundary conditions and temperature or heat flux obtained in Eq. (22) in a set of M points at the boundary of the square solid. Then this functional is minimised as in the least square approach to determine $C_k^{(1)}$ and $C_k^{(2)}$. Thus, the complex potentials (22) are obtained explicitly. Using Eqs (1) and (22) it is then easy to plot temperature change in the cross-section of a

square solid depending on the distance to the interface (for instance, Fig. 4 depicts plot for HCI with $\mu_0/\mu_0^* = 1$). Since, on the boundary $y = \frac{H}{2}$ temperature is $\theta = x^2$, then the graph of temperature change for $y > 0$ is parabolic (Fig. 4). The $y < 0$ plot shows that the temperature change is a linear function of coordinate, since we selected very high-temperature conductivity of the interface, and thus the temperature of the latter should be constant.

The same results were obtained using developed modified boundary elements method, which once again confirms its correctness.

Example 3. Consider the problem of plane strain for a thermomagnetoelectroelastic anisotropic bimaterial consisting of two half-spaces. It contains a rectilinear elastic isotropic thermally insulated electro- and magnetically permeable inclusion of finite length $2a$. For its modelling the coupling principle for continua of different dimension is used [10]. In this example, it is assumed that the coefficients of linear thermal expansion of the inclusion material are zero. Its cross section is perpendicular to the bimaterial boundary (Fig. 5). One inclusion tip is located.in the half-space $x_2 > 0$, and the other in the half-space $x_2 < 0$. The singularity at the point of intersection of the inclusion with the material interface is not accounted for. The centre of inclusion coincides with the origin. Inclusion thickness is $h = 0{,}01a$, and its relative rigidity is $k = \frac{G_i}{C_{11}}$.

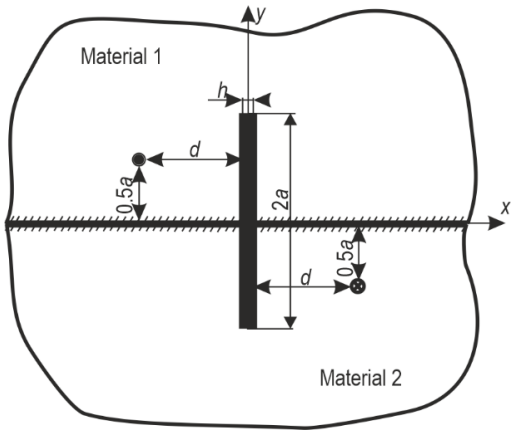

Fig. 5. Scheme of the problem for a thermomagnetoelectroelastic anisotropic bimaterial containing a thin inhomogeneity

The heat source of intensity q is located in the half-space $x_2 > 0$ at a distance of $0{,}5a$ to the interface; heat drain of the same intensity q is located in the half-space $x_2 < 0$ also, at a distance of $0{,}5a$ to the interface antisymmetrically.

Two problems are considered:

I) both bimaterial components are made of barium titanate ($BaTiO_3$);

II) the component $x_2 > 0$ is made of barium titanate, and $x_2 < 0$ of cadmium selenide (CdSe).

According to [18], the properties of $BaTiO_3$ are as follows:
elastic moduli: $C_{11} = C_{33} = 150,\ C_{22} = 146,\ C_{12} = C_{13} = C_{23} = 66,\ C_{44} = C_{66} = 44,\ C_{55} = 42$;
piezoelectric constants: $e_{21} = e_{23} = -4.35,\ e_{22} = 17{,}5,\ e_{16} = e_{34} = 11{,}4$;
dielectric constants: $\kappa_{11} = 9{,}86775,\ \kappa_{22} = 11{,}151$;
heat conduction coefficients: $k_{11} = k_{22} = 2.5$;
thermal expansion coefficients: $\alpha_{11} = 8.53 \cdot 10^{-6},\ \alpha_{22} = 1.99 \cdot 10^{-6}$; pyroelectric constants: $\lambda_2 = 13{,}3 \cdot 10^{-6}$.
The properties of CdSe are as follows [19]:
elastic moduli: $C_{11} = C_{33} = 74.1,\ C_{22} = 83.6,\ C_{12} = C_{23} = 39.3,\ C_{13} = 45.2,\ C_{44} = C_{66} = 13.17,\ C_{55} = 14.45$;
piezoelectric constants: $e_{21} = e_{23} = -0{,}160,\ e_{22} = 0{,}347,\ e_{16} = e_{34} = -0{,}138$;
dielectric constants: $\kappa_{11} = 0.0826,\ \kappa_{22} = 0{,}0903$;
heat conduction coefficients: $k_{11} = 1,\ k_{22} = 2.5$;
thermal expansion coefficients: $\beta_{11} = \beta_{33} = 0{,}621,\ \beta_{22} = 0{,}551$;
pyroelectric constants: $\chi_2 = -2{,}94 \cdot 10^{-6}$.

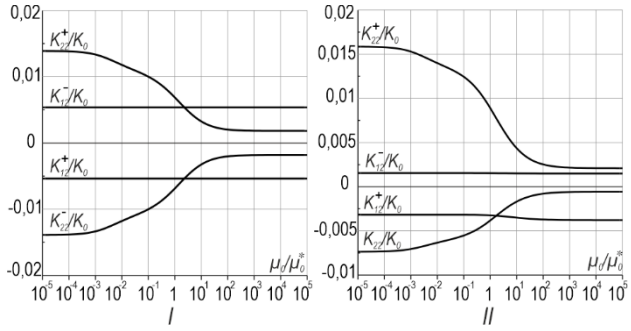

Fig. 6. Dependence of dimensionless generalised SIFs of the inclusion in an infinite body on the parameter of the interface μ_0

The plots in Fig. 6 show the dependence of the dimensionless stress intensity factors on the thermal conductivity parameter of the interface μ_0. All calculations were performed by the above-mentioned method of boundary elements [6], [8]. 20 boundary elements were used to model the inclusion surface. With a further increase in the number of elements, the results obtained differ by <0.5%. Generalised SIFs and thermal conductivity parameter are normalised by $K_0 = q\beta_{11}\sqrt{\pi a}/k_{11}$ and $\mu_0^* = ak_{11}$, respectively. Here k_{11} and β_{11} are coefficients of $BaTiO_3$.

It is noticed that in the first case in Fig. 6 (*I*), when the components of the matrix are made of the same materials with geometric symmetry of the problem and asymmetry of temperature load, the values of stress intensity factors at opposite tips of the inclusion are expected to be the same in magnitude and opposite in sign. The maximum are dimensionless SIFs $K_{22}^+/K_0 = K_{22}^-/K_0$, $\approx 0{,}014$ for the high-temperature conducting interface at $\mu_0/\mu_0^* = 10^{-5}$.

When half-spaces have different properties but the same geometry of the problem and the same heat load (Fig. 6 (II)), the symmetry of the solution is obviously not observed. Since the material of the half-space $x_2 > 0$ is the same as in the previous case, the values of the SIFs at the inclusion tip located in this half-plane will change very little. However, at the inclusion tip, which is located in the lower half-space, the change in coefficients is more noticeable: when $\mu_0/\mu_0^* = 10^{-5}$ K_{22}^-/K_0 changes from 0.014 to 0.0075, and K_{12}^-/K_0 from 0.005 to 0.002.

Example 4. Now consider the bimaterial containing two identical inclusions that are perpendicular to the boundary. Their properties are the same as in the previous example. They are placed at a distance d to the axis x_2.The heat source and drain of the same magnitude are located at a distance of $0{,}5a$ to the material interface and at the distance of $2d$ to the axis x_2 (Fig. 7).

As in the previous problem, we study the dependence of stress intensity factors on the thermal conductivity parameter of the interface μ_0, $(\mu_0^* = \alpha k_{11})$.

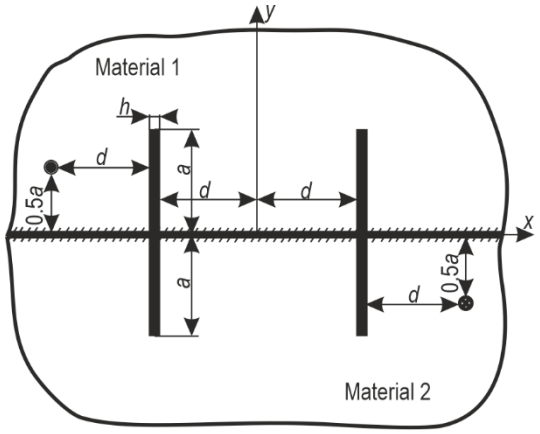

Fig. 7. Scheme of the problem for thermoelastic anisotropic bimaterial with two inclusions

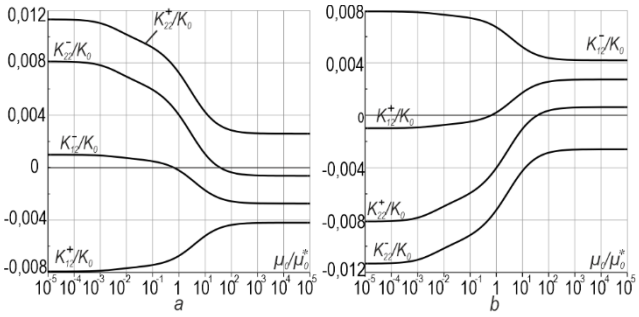

Fig. 8. Dependence of dimensionless generalised SIFs of two inclusions in an infinite body on the parameter of the interface μ_0, when the components are made of the same materials

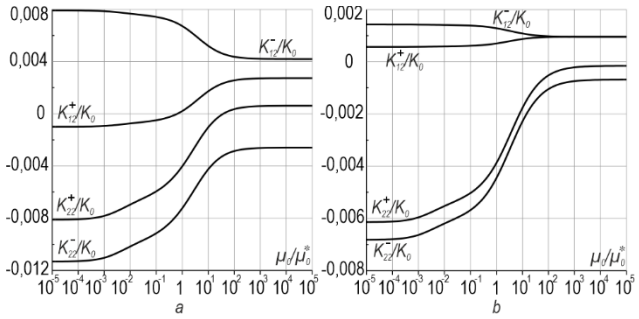

Fig. 9. Dependence of dimensionless generalised SIFs of two inclusions in an infinite body on the parameter of the interface μ_0, when the components are made of different materials

The plots (Fig. 8) show the values of generalised SIFs for the (a) first and (b) second inclusions, when the components of the matrix are made of the same materials.

Due to the fact that the inclusions are identical in their properties and located symmetrically about the axes x_2 and x_1, and the materials of the components have the same properties, the plots for both inclusions have a similar behaviour and differ only in sign. As in the previous problem, the maximum values of $K_{22}^+/K_0 = 0{,}011$ were obtained for $\mu_0/\mu_0^* = 10^{-5}$

Somewhat different results are observed in the case when the component $x_2 < 0$ of the bimaterial is made of a material, whose properties are different from $x_2 > 0$.

Fig. 9(a) shows that in this case the values of SIFs at the vertex of the first inclusion have undergone significant changes in comparison with the matrix of Fig. 8(a). The maximum value K_{22}^+/K_0 increased from 0.011 to 0.014; and K_{22}^-/K_0 from 0.008 to 0.012. The values K_{12}^-/K_0 have also increased.

By contrast, at the tip of the second inclusion, the values of SIFs decreased. Fig. 9(b) shows that the maximum value K_{22}^-/K_0 decreased from 0.011 to 0.0078; K_{22}^+/K_0 from 0.008 to 0.0061. Also, at the upper and lower ends of the second inclusion approach the value of 0.001 at $\mu_0/\mu_0^* = 10^2$.

6. CONCLUSION

A mathematical model of a thermagnetoelectroelastic bimaterial solid with a high-temperature conducting coherent interface and a perfect magnetoelectromechanical contact of components has been developed, which in turn may contain thin deformable inclusions. In a closed form, purely boundary integral equations of the formulated problem are derived. That is, equations in which there is no need to take into account the integrals along the interface; thus, the boundary element mesh is required only for the boundary of the composite body and the midline of the thin inclusions.

The method can be extended to account for inclusions at the bimaterial interface; however, the oscillating singularity at its tip should be accounted for, which is beyond the scope of the present publication. Nevertheless, the present paper accounts for imperfect interface, which physically means a thin layer of different properties on the bimaterial interface, which is very important in practical applications.

The use of the obtained integral equations in combination with the boundary element method allows to solve several new problems for bimaterials consisting of the same and different anisotropic thermomagnetoelectroelastic materials, as well as containing thin deformable inclusions. Graphical dependences of generalised SIFs on the thermal conductivity parameter are derived. The obtained results show that the high thermal conductivity interface significantly affects the stress fields at the vertices of thin inclusions.

All this allows to state that the developed method allows to solve with high accuracy the problem of thermomagnetoelasticity for bimaterial solids with a high-temperature conducting interface with thin ribbon-like deformable inclusions or cracks, which has not been possible so far using traditional numerical approaches.

REFERENCES

1. Kaessmair S, Javili A, Steinmann P. Thermomechanics of solids with general imperfect coherent interfaces. Archive of Applied Mechanics. 2014;84: 1409-1426. https://doi.org/10.1007/s00419-014-0870-x
2. Benvensite Y. A general interface model for a three-dimensional curved thin anisotropic interphace between two anisotropic media. Journal of the Mechanics and Physics of Solids. 2006;54: 708-734. https://doi.org/10.1016/j.jmps.2005.10.009
3. Pasternak I, Pasternak R, Sulym H. Boundary integral equations and Green's functions for 2D thermoelectroelastic biomaterial. Engineering Analysis with Boundary Elements. 2014;48: 87-101. https://doi.org/10.1016/j.enganabound.2014.06.010
4. Pasternak I, Pasternak R, Sulym H. 2D boundary element analysis of defective thermoelectroelastic bimaterial with thermally imperfect but mechanically and electrically perfect interface. Engineering Analysis with Boundary Elements. 2015;61: 194-206. https://doi.org/10.1016/j.enganabound.2015.07.012

5. Muskhelishvili NI. Singular Integral Equations: Boundary Problems of Function Theory and Their Application to Mathematical Physics. First Edition. Mineola: Dover Publications; 2008.
6. Hwu C. Anisotropic elastic plates. London: Springer; 2010.
7. Ting TC. Anisotropic elasticity: theory and applications. New York: Oxford University Press; 1996.
8. Pasternak I. Boundary integral equations and the boundary element method for fracture mechanics analysis in 2D anisotropic thermoelasticity. Engineering Analysis with Boundary Elements. 2012;36(12): 1931-41. https://doi.org/10.1016/j.enganabound.2012.07.007
9. Pasternak I. Coupled 2D electric and mechanical fields in piezoelectric solids containing cracks and thin inhomogeneities. Engineering Analysis with Boundary Elements. 2011;23: 678-90. https://doi.org/10.1016/j.enganabound.2010.12.001
10. Sulym GT. Bases of the Mathematical Theory of Thermoelastic Equilibrium of Deformable Solids with Thin Inclusions [inUkrainian]. Lviv: Dosl.-Vyd. Tsentr NTSh; 2007.
11. Pan E, Amadei B. Boundary element analysis of fracture mechanics in anisotropic bimaterials. Engineering Analysis with Boundary Elements. 1999;23: 683-91. https://doi.org/10.1016/S0955-7997(99)00018-1
12. Wang X, Pan E. Thermal Green's functions in plane anisotropic bimaterials with spring-type and Kapitza-type imperfect interface. Acta Mechanica et Automatica. 2010;209: 115-128. https://doi.org/10.1007/s00707-009-0146-7
13. Sladek J, Sladek V, Wuensche M, Zhang, Ch. Analysis of an interface crack between two dissimilar piezoelectric solids. Engineering Fracture Mechanics. 2012;89: 114-27. https://doi.org/10.1016/j.engfracmech.2012.04.032
14. Wang TC, Han XL. Fracture mechanics of piezoelectric materials. International journal fracture mechanics. 1999;98: 15-35. https://doi.org/10.1023/A:1018656606554
15. Qin QH. Green's function and boundary elements of multifield materials. Oxford: Elsevier Science; 2007.
16. Yang J. Special topics in the theory of piezoelectricity. London: Springer; 2009.
17. Pasternak I, Pasternak R, Sulym H. A comprehensive study on the 2D boundary element method for anisotropic thermoelectroelastic solids with cracks and thin inhomogeneities, Engineering Analysis with Boundary Elements. 2013;37(2): 419-33. https://doi.org/10.1016/j.enganabound.2012.11.002
18. Dunn ML. Micromechanics of coupled electroelastic composites: Effective thermal expansion and pyroelectric coefficients. Journal of Applied Physics. 1993;73: 5131-40. https://doi.org/10.1063/1.353787
19. Berlincourt D, Jaffe H, Shiozawa LR. Electroelastic properties of the sulfides, selenides, and tellurides of zinc and cadmium. Physical Review. 1963;129: 1009-17. https://doi.org/10.1103/PhysRev.129.1009

Heorhiy Sulym: https://orcid.org/0000-0003-2223-8645
Andrii Vasylyshyn: https://orcid.org/0000-0002-5703-6894
Iaroslav Pasternak: https://orcid.org/0000-0002-1732-0719